

## Synthesis and Solid-State, Solution, and Luminescence Properties of Near-Infrared-Emitting Neodymium(3+) Complexes Formed with Ligands Derived from Salophen

by Hyounsoo Uh<sup>a</sup>), Paul D. Badger<sup>a</sup>), Steven J. Geib<sup>a</sup>), and Stéphane Petoud<sup>\*a</sup>)<sup>b</sup>)

<sup>a</sup>) Department of Chemistry, University of Pittsburgh, 219 Parkman Ave., Pittsburgh, PA 15260, USA  
(phone: +1-412-624-8210; fax: +1-412-624-8611; e-mail: spetoud@pitt.edu)

<sup>b</sup>) Centre de Biophysique Moléculaire, CNRS, Rue Charles-Sadron, F-45071 Orléans Cedex 2  
(phone: +33(0)238255652; fax: +33(0)238631517; e-mail: stephane.petoud@cnrs-orleans.fr)

Dedicated to Professor *Jean-Claude Bünzli* on the occasion of his 65th birthday

---

A series of free ligands, H<sub>2</sub>L<sup>1</sup>, H<sub>2</sub>L<sup>2</sup>, H<sub>2</sub>L<sup>3</sup>, and H<sub>2</sub>L<sup>4</sup>, designed for the coordination and sensitization of near-infrared(NIR)-emitting Nd<sup>3+</sup> were synthesized by modifying the salophen *Schiff* base with different numbers and locations of Br-substituents. The nature of the Nd<sup>3+</sup> complexes in solution was determined to be [ML<sub>2</sub>]<sup>-</sup> by spectrophotometric titrations as an indication that the different substituents do not affect significantly the nature of the formed species. The structures were determined in the solid phase from X-ray diffraction experiments. The stoichiometries and structures in the solid state are different from those observed in solution. We established that the structures in the solid state can be partially controlled by the crystallization conditions. The ligands L<sup>1</sup>–L<sup>4</sup> have the ability to sensitize Nd<sup>3+</sup> through intramolecular energy transfer from the ligand to the metal ion. We quantified that the numbers and locations of Br-substituents control the emitted luminescence intensity of the complex by the heavy-atom effect.

---

**Introduction.** – There is a continuously growing interest for the properties of near-infrared(NIR)-luminescent lanthanide complexes [1–44]. As examples of applications, NIR lanthanide luminescence can be used in NIR organic light-emitting diode technology [45] or in telecommunication where the electronic structure of lanthanide ions such as Er<sup>3+</sup>, Nd<sup>3+</sup>, and Ho<sup>3+</sup> can be used as the active material for optical amplification of NIR signals [46]. The use of NIR luminescence is also a promising approach for biological imaging because NIR photons have less interference with biological materials: most of biological molecules located in the skin, blood, and tissues have lower absorption [47][48] in the NIR region, allowing photons to penetrate deeply into tissues for noninvasive detection. Since the autofluorescence from biological tissue is mainly located in the violet–blue region [49], imaging in the NIR region also has an added advantage for the detection sensitivity due to an improved signal-to-noise ratio, the background emission in the NIR being lower [48]. An additional advantage of NIR imaging is the limited scattering of NIR photons in comparison to VIS photons that result in improved image resolution. As the intensity of scattered light is proportional to 1/λ<sup>4</sup>, the longer wavelength of NIR light has reduced scattering, which results in the higher resolution of the obtained image [50].

NIR-Luminescent lanthanide complexes also have the advantages that are common to all lanthanides, including photostability (allowing the use of the luminescence for long experiments) [51], sharp emission bands (allowing spectral discrimination) [52], and long luminescent lifetimes (allowing temporal discrimination) [53].

Due to their electronic structure, free lanthanide cations have low absorption coefficients and long intrinsic luminescence lifetime [2][3]. To generate a sufficient number of photons allowing sensitive detection, lanthanide cations must be sensitized with a suitable antenna that possesses the appropriate electronic structure [54] and that can sufficiently protect the cation from high-energy vibrations to prevent the nonradiative deactivation of the lanthanide luminescence.

To achieve adequate emission intensity from lanthanide ions, the sensitizers or antennae should fulfill several requirements: 1) the sensitizers have to form a complex with lanthanide ions that does not dissociate easily, which typically have a high coordination number comprised between 8 to 10; 2) the energy levels of the triplet states of the sensitizers must match the accepting energy level of the lanthanide ions to achieve a good energy transfer; 3) the sensitizer-ligand has to provide good protection for lanthanide ions from nonradiative deactivation through solvent-molecule vibrations. In addition, the sensitizer should be easy to modify to control chemical and/or photophysical properties of the resulting luminescent lanthanide complex.

Several sensitizers or antennae have been described for the sensitization of NIR-emitting lanthanide cations [1–44]. The number of antennae for NIR-emitting lanthanides is still moderate, and it is interesting to test additional systems to broaden our understanding of the relationship between electronic structure of the antenna and luminescence properties of the resulting complexes.

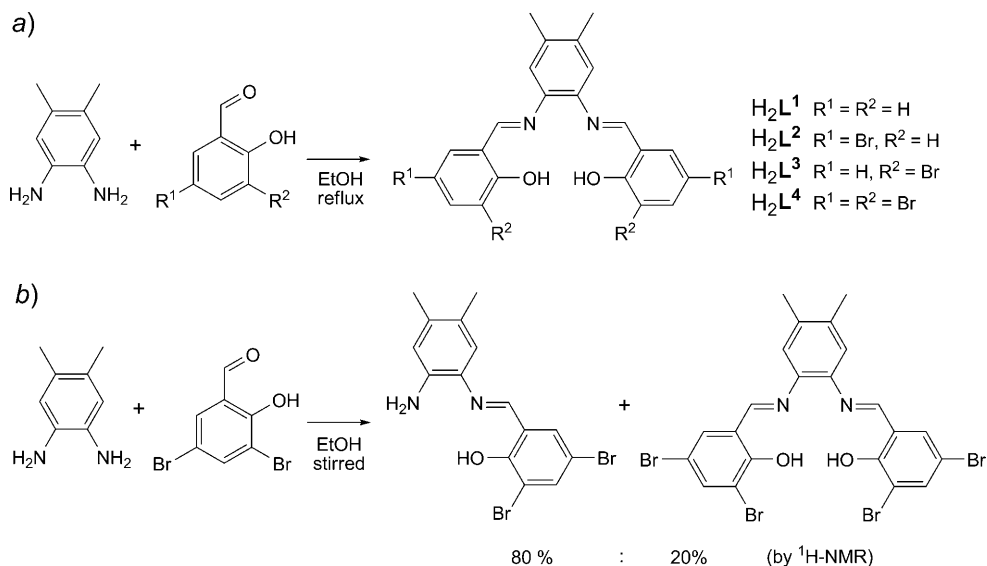
In this work, we investigated a system based on the ligand salophen (= 2,2'-[1,2-phenylenebis(nitrilomethylidene)]bis[phenolato]<sup>2-</sup>) where different substituents can be rapidly attached to evaluate their effect on the solution behavior, solid-state structure, and luminescence properties of these complexes.

Metal complexes formed with *Schiff* ligands have occupied an important role in coordination chemistry for over half a century [55]. Salen, ethylenediamine-bridged modified salicylaldehydes, and salophen, 1,2-phenylenediamine-bridged modified salicylaldehydes, have been extensively employed because of their stability resulting from the conjugated structure, the pre-organized tetradentate coordination geometry, the simplicity of synthesis and the facile modification of their structures. Salophen derivatives can act as good sensitizer-ligands for luminescent lanthanide cations because this family of ligands can fulfill the specific requirements for lanthanide luminescence. The planar and rigid ligands have tetradentate coordination geometry which can be hypothesized to lead to the formation of [ML<sub>2</sub>]<sup>-</sup> complexes with lanthanide ions to fulfill their coordination-number requirements. The energy of the triplet state of the unsubstituted salophen chromophoric ligand has been reported to be located at 17510 cm<sup>-1</sup> [56]. This energy of electronic level is suitable for a rapid and irreversible intramolecular energy transfer to NIR-emitting lanthanide ions such as Nd<sup>3+</sup> that has one main accepting level located at 11300 cm<sup>-1</sup>. Another advantage of the salophen moiety is the easy and versatile modification of its structure. A large number of derived ligands possessing different substituents can be rapidly synthesized in few steps. A family of ligands possessing a variety of substituents is important for

the systematic study and control of the photophysical properties of lanthanide complexes.

**Results and Discussion.** – *Synthesis of Ligands and Complexes.* The salophen-type ligands  $H_2L^1$ ,  $H_2L^2$ ,  $H_2L^3$ , and  $H_2L^4$  can be easily synthesized by condensation of two equiv. of a salicylaldehyde and one equiv. of benzene-1,2-diamine in refluxing EtOH (*Scheme, a*). This reaction is fast and, in most cases, quantitative, with the heating of the reaction mixture being essential. Without heating, the major product that was obtained was a *Schiff* base with only one amine group condensed with the salicylaldehyde (bidentate system; *Scheme, b*). In addition to the effect of the temperature, the formation and structure of *Schiff* bases is also controlled by the number of equivalents of aldehydes and amines. *MacLachlan* and co-workers reported the syntheses of *Schiff* bases with various ratios of aldehyde/amine from the same dialdehyde and diamine [57]. All the diamines and aldehydes used in this work were commercially available, except for 3-bromosalicylaldehyde. The latter was synthesized from bromophenol and paraformaldehyde in the presence of magnesium chloride [58].

Scheme. Condensation Reaction of One Benzene-1,2-diamine with Two Salicylaldehydes and Structures of the Chromophoric Ligands Used in This Work



The syntheses of the different  $[NdL_2]^-$  complexes were carried out by the reaction of 2 equivalents of salophen-type ligand  $H_2L$  and 1 equiv. of  $Nd(OTf)_3 \cdot 6 H_2O$ . Depending on the solubility of the ligand, MeCN or a mixture THF/MeCN was used as solvent. One and a half equiv. of NaOH in MeOH was used as a base to ensure complete deprotonation of the ligand. The Nd complexes were isolated by solvent evaporation followed by precipitation.

*Crystal Structure of the Complexes.* To grow X-ray-diffraction-quality samples of  $[Nd(L^x)]$  ( $x = 1-4$ ), the following method was used: To a suspension of a ligand  $H_2L^x$

dissolved in MeOH, an excess (*ca.* 500–600 equiv.) of Et<sub>3</sub>N was added. A half equivalent of Nd(OTf)<sub>3</sub>·6 H<sub>2</sub>O was then added to the ligand solution, and hexane was diffused slowly into this solution. Crystals of [Nd<sub>2</sub>(L<sup>1</sup>)<sub>3</sub>] and [Nd(L<sup>4</sup>)<sub>2</sub>]<sup>−</sup> were obtained with this method and analyzed with X-ray diffraction.

The crystal of the complex with L<sup>4</sup> has the formula Et<sub>3</sub>NH<sup>+</sup>[Nd(L<sup>4</sup>)<sub>2</sub>]<sup>−</sup>. As shown in Fig. 1, a, the molecular structure of the obtained crystals can be described as a double-decker sandwich (for selected bond lengths and angles, see Table 1). There is one previous example of a lanthanide complex with a salophen-derived ligand which adopts such a double-decker sandwich conformation [59]. This complex is formed by the coordination of one Ce<sup>4+</sup> as metal cation with two salophen as ligand. It is interesting to note that the lanthanide cation coordinated in this complex has a different oxidation state and, therefore, cannot be considered as similar. In addition to the difference in charge, Ce<sup>4+</sup> has a significantly different effective ionic radius: 0.97 Å for Ce<sup>4+</sup> vs. 1.109 Å for Nd<sup>3+</sup>, both calculated according to Shannon for eight coordinated cations) [60].

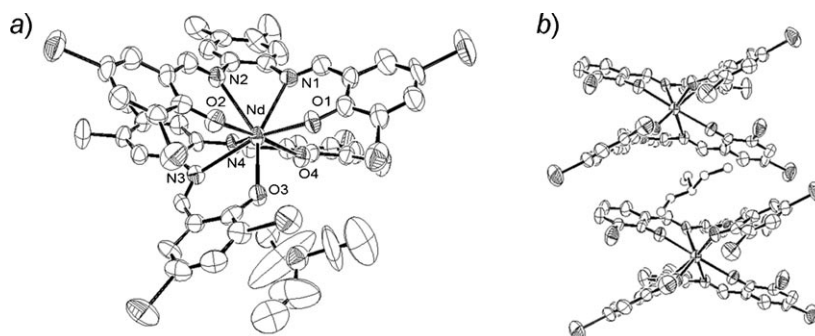


Fig. 1. a) Molecular structure of [Nd(L<sup>4</sup>)<sub>2</sub>]<sup>−</sup> with Et<sub>3</sub>NH<sup>+</sup> as counter cation. b) Et<sub>3</sub>NH<sup>+</sup> in the crystal-packing structure of Et<sub>3</sub>NH<sup>+</sup>[Nd(L<sup>4</sup>)<sub>2</sub>]<sup>−</sup>. Arbitrary atom numbering.

Table 1. Selected Bond Lengths [Å] and Angles [°] in Et<sub>3</sub>NH[Nd(L<sup>4</sup>)<sub>2</sub>]. For atom numbering, see Fig. 1.

Nd–O(1)	2.327(6)	O(1)–Nd–O(2)	94.9(2)
Nd–O(2)	2.353(6)	O(2)–Nd–N(2)	68.0(2)
Nd–O(3)	2.367(6)	N(2)–Nd–N(1)	60.6(2)
Nd–O(4)	2.345(6)	N(1)–Nd–O(1)	69.6(2)
Nd–N(1)	2.629(7)	O(3)–Nd–O(4)	91.3(2)
Nd–N(2)	2.672(8)	O(4)–Nd–N(4)	66.8(2)
Nd–N(3)	2.678(7)	N(4)–Nd–N(3)	60.4(2)
Nd–N(4)	2.689(8)	N(3)–Nd–O(3)	68.6(2)

Two salophen-type ligands coordinate each to the Nd<sup>3+</sup> center in a tetradentate fashion. The salicylidene arms are bent toward the exterior of the molecule. For each salophen-type ligand coordinated to Nd<sup>3+</sup>, one 5-membered ring, Nd–N(1)–C(8)–C(13)–N(2) and two six-membered rings, Nd–N(1)–C(7)–C(6)–C(1)–O(1) and

<sup>1</sup>) CCDC-733475 and -733476 contain the supplementary crystallographic data for this work. These data can be obtained free of charge via [http://www.ccdc.cam.ac.uk/data\\_request/cif](http://www.ccdc.cam.ac.uk/data_request/cif).

Nd–N(2)–C(14)–C(15)–C(20)–O(2), are formed (Fig. 2, a). The salicylidene arms are bent to make these three rings as planar as possible. Since the  $[\text{Nd}(\mathbf{L}^4)]^-$  complex has a net  $-1$  charge,  $\text{Et}_3\text{NH}^+$  acts as a counter cation. In the crystal-packing structure (Fig. 1, b),  $\text{Et}_3\text{NH}^+$  is located in the space between two molecules of  $[\text{Nd}(\mathbf{L}^4)]^-$ . The presence of  $\text{Et}_3\text{NH}^+$  may be another factor contributing to the bending of the salophen-type ligands. Molecules and ions are closely packed together to have minimal energy in a crystal. The bent salicylidene arms can provide the space to accommodate the relatively larger  $\text{Et}_3\text{NH}^+$  cation in the crystal-packing structure of  $\text{Et}_3\text{NH}^+[\text{Nd}(\mathbf{L}^4)]^-$ .

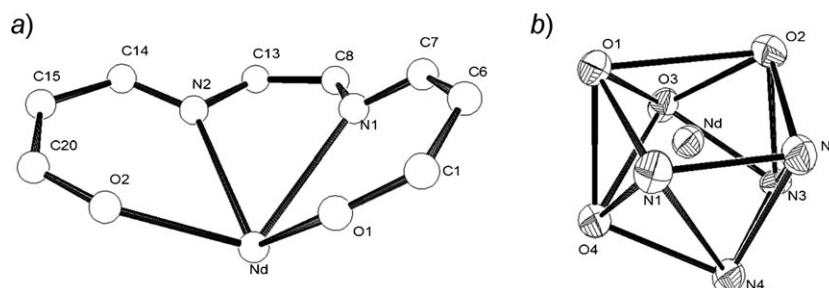


Fig. 2. a) Five- and six-membered rings formed by coordination of the ligand  $\mathbf{L}^4$  to  $\text{Nd}^{3+}$  and b) coordination polyhedron around  $\text{Nd}^{3+}$  in  $\text{Et}_3\text{NH}^+[\text{Nd}(\mathbf{L}^4)]^-$ . Arbitrary atom numbering.

When viewed from the orthogonal point of view with respect to the salophen plane, the two salophen-type ligands are oriented in a staggered fashion. The coordination environment around the  $\text{Nd}^{3+}$  cation is close to a square antiprism geometry (Fig. 2, b). Atoms O(1), O(2), N(2), and N(1) form a nearly planar coordination ring, and atoms O(3), O(4), N(4), and N(3) also form a nearly planar coordination ring. However, these coordination rings are trapezoids: the O–O segments (3.37–3.45 Å) are longer than the N–N segments (2.68–2.70 Å). Because two N-atoms N(1) and N(2) (or N(3) and N(4), resp.) are attached to the same phenylene moiety, there is limited flexibility around the N-atoms, but the relatively more flexible salicylidene arms allow the O–O distances to be increased. The Nd–O bonds are shorter than the Nd–N bonds. This situation induces the two planes O(1)–O(2)–N(2)–N(1) and O(3)–O(4)–N(4)–N(3) being not perfectly parallel.

The structure of the  $[\text{Nd}_2(\mathbf{L}^1)_3]$  complex is shown in Fig. 3. Thus an  $[\text{M}_2\text{L}_3]$  structure, *i.e.*,  $[\text{Nd}_2(\mathbf{L}^1)_3] \cdot \text{MeOH}$  was isolated (for selected bond lengths and angles, see Table 2). Similar types of triple-decker and tetra-decker  $\text{Tb}^{3+}$  complexes of salophen derivatives have been reported previously [61].

It is interesting to note that the three ligands are not located on the same axis.  $\mathbf{L}^1(1)$  and Nd(1) are out of the line formed by the (center of  $\mathbf{L}^1(2)$ )–Nd(2)–(center of  $\mathbf{L}^1(3)$ ). The two N-atoms of  $\mathbf{L}^1(2)$  (N(3) and N(4)) are only coordinated to Nd(2), and have no coordination to Nd(1). Because an N-atom has only one lone pair to coordinate to the metal ion, while an O-atom has two or three lone pairs, an N-atom can bind to only one metal ion. Thus Nd(1) cannot be located on the center of  $\mathbf{L}^1(2)$ , and it is coordinated by the two O-atoms of  $\mathbf{L}^1(2)$  (O(3) and O(4)) and the two O-atoms (O(1) and O(2)) and the two N-atoms (N(1) and N(2)) of  $\mathbf{L}^1(1)$ . To fill the remaining coordination site, solvent MeOH is bound to Nd(1) in the first sphere of coordination.

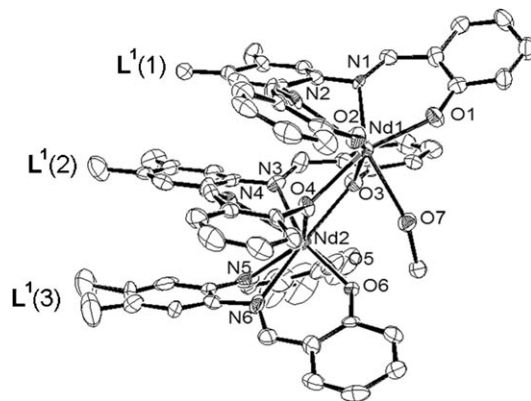


Fig. 3. Molecular structure of  $[Nd_2L^1_3] \cdot MeOH$ . Arbitrary atom numbering.

Table 2. Selected Bond Lengths [ $\text{\AA}$ ] and Angles [ $^\circ$ ] in  $[Nd_2(L^1)_3] \cdot MeOH$ . For atom numbering, see Fig. 3.

Nd(1)–O(1)	2.271(8)	O(1)–Nd(1)–O(2)	97.2(3)
Nd(1)–O(2)	2.253(8)	O(2)–Nd(1)–N(2)	72.1(3)
Nd(1)–N(1)	2.545(9)	N(2)–Nd(1)–N(1)	63.4(3)
Nd(1)–N(2)	2.552(10)	N(1)–Nd(1)–O(1)	71.6(3)
Nd(1)–O(3)	2.476(8)	O(3)–Nd(1)–O(4)	69.7(3)
Nd(1)–O(4)	2.409(8)	O(3)–Nd(1)–O(7)	75.8(3)
Nd(1)–O(7)	2.459(10)	O(7)–Nd(1)–O(4)	75.8(3)
Nd(2)–O(3)	2.409(8)	O(3)–Nd(2)–O(4)	70.8(3)
Nd(2)–O(4)	2.410(8)	O(4)–Nd(2)–N(4)	68.1(3)
Nd(2)–N(3)	2.598(10)	N(4)–Nd(2)–N(3)	60.4(3)
Nd(2)–N(4)	2.679(10)	N(3)–Nd(2)–O(3)	69.4(3)
Nd(2)–O(5)	2.313(8)	O(5)–Nd(2)–O(6)	90.9(3)
Nd(2)–O(6)	2.365(8)	O(6)–Nd(2)–N(6)	71.2(3)
Nd(2)–N(5)	2.573(11)	N(6)–Nd(2)–N(5)	62.3(3)
Nd(2)–N(6)	2.575(10)	N(5)–Nd(2)–O(5)	70.0(4)

The same coordination pattern (two salophen-type ligands form an eight-coordinated metal complex and additional metal ions and salophen-type ligands are located out of the axis providing 7- or 8-coordination sites with one or two solvent molecules) are observed in reported triple-decker or tetra-decker structures of  $Ln^{3+}$  complexes [61].

*Determination of the Nature and Stability Constants of the  $Nd^{3+}$  Complexes by Batch Spectrophotometric Titrations.* To confirm the nature of the complexes formed between  $Nd^{3+}$  and the different ligands in solution, batch spectrophotometric titrations were performed in DMSO. Two methods were employed to fully deprotonate the ligands prior to titration to ensure the complete formation of the complexes during the titration process. In the first method, 2 equiv. of KOH per equiv. of ligand were added to a suspension of ligand in MeOH. Upon addition, the solution became clear suggesting the deprotonation of the ligand. After evaporation of the solvent, the potassium salt of the ligand was used as starting material for the creation of the solutions for the batch

titration. The other method was the addition of an organic base such as triethylamine ( $\text{Et}_3\text{N}$ ) into the titration solutions. The solution can then be used as such and corresponds to a deprotonation of the ligand *in situ*. This second method has an advantage since the instability of the potassium salt of the ligand and the undesirable re-protonation of the ligand can be avoided.

Batch titrations of three salophen-type ligands,  $\text{H}_2\text{L}^1$ ,  $\text{H}_2\text{L}^3$ , and  $\text{H}_2\text{L}^4$ , with  $\text{Nd}^{3+}$  were carried out varying metal/ligand ratios from 0 : 1 to 2 : 1 equiv. For  $\text{H}_2\text{L}^1$ , KOH was used as a base and deprotonation was done prior to the titration. For  $\text{H}_2\text{L}^3$  and  $\text{H}_2\text{L}^4$ ,  $\text{Et}_3\text{N}$  was used as a base and deprotonation was achieved *in situ*. The titration of  $\text{H}_2\text{L}^1$  with  $\text{Nd}^{3+}$  in the presence of  $\text{Et}_3\text{N}$  as a base was also tested, but no meaningful results were obtained. This negative result was attributed to  $\text{Et}_3\text{N}$  being not basic enough to fully deprotonate  $\text{H}_2\text{L}^1$  (*vide infra*). This situation can be explained since  $\text{H}_2\text{L}^1$  does not incorporate electron-withdrawing Br groups that stabilize the basic form of the ligand. The plots of results are summarized in Fig. 4, where the absorbance of the solutions at chosen wavelengths are plotted against the metal/ligand ratios. In all three cases, a breaking point appears at a metal/ligand ratio of *ca.* 1 : 2, indicating the formation of the  $[\text{ML}_2]$  complex for all three ligands.

The stability constants corresponding to the formation of the complexes between the ligands  $\text{L}^1$ ,  $\text{L}^3$ , and  $\text{L}^4$  with  $\text{Nd}^{3+}$  were calculated from these titrations with the data-analysis software SPECFIT [62]. The best fits were obtained with a model corresponding to the successive formation of  $[\text{ML}_1]$  and  $[\text{ML}_2]$  complexes. Convergence of the fitting process for the calculation of the  $\log K_2$  value was possible when the values of  $\log K_1$  were fixed to values comprised between 9 and 12, and the obtained values of  $\log K_2$  remained systematically unchanged. This observation can be explained by the very high stability of the  $[\text{ML}_1]$  species formed in solution and has been observed for other NIR-emitting lanthanide complexes [43].  $\log K_2$  stability-constant values of  $6.4 \pm 0.3$ ,  $6.8 \pm 0.4$ , and  $7.2 \pm 0.3$  were obtained after fitting the data obtained from  $\text{M}/(\text{L}^1)_2$ ,  $\text{M}/(\text{L}^3)_2$ , and  $\text{M}/(\text{L}^4)_2$  titrations, respectively.

From these data, we can observe that the presence of the Br-substituents on the salophen moiety do not have a major contribution on the stability of the different  $[\text{ML}_2]$  complexes formed in solution. With these titration experiments, we were able to confirm that all the studied salophen-type ligands form  $[\text{ML}_2]$  complexes when treated with  $\text{Nd}^{3+}$  cation in solution.

It is interesting to note that the stoichiometry of this complex which is 1 : 2 in solution is different in the solid phase. Since the net charge of the  $[\text{ML}_2]$  complex is  $-1$ , a counter cation must be present for the formation of the  $[\text{ML}_2]$  complex. No counter cation is present in the structure of  $[\text{Nd}_2(\text{L}^1)_3]$ , while  $\text{Et}_3\text{NH}^+$  acts as counter cation in the structure of  $[\text{Nd}(\text{L}^4)_2]^-$ . In the absence of a counter cation, the reaction between the trivalent  $\text{Nd}^{3+}$  and divalent  $\text{L}^{2-}$  results in the formation of a complex with a  $[\text{M}_2\text{L}_3]$  formula. This result indicates that  $\text{Et}_3\text{N}$  cannot act as a base for the deprotonation of the ligand  $\text{H}_2\text{L}^1$  when present in solution with  $\text{Nd}^{3+}$  during the crystal-growth process. Investigation of the acidities of the salophen-type ligands provided more insightful information of whether  $\text{Et}_3\text{N}$  is basic enough to fully deprotonate the ligands described in this work. A UV/VIS absorbance analysis was carried out to compare the relative acidities of the salophen-type ligands  $\text{H}_2\text{L}^1$ ,  $\text{H}_2\text{L}^2$ ,  $\text{H}_2\text{L}^3$ , and  $\text{H}_2\text{L}^4$  in DMSO, prior and after addition of an excess of  $\text{Et}_3\text{N}$  (Fig. 5). The absorbance spectra of  $\text{H}_2\text{L}^3$  and  $\text{H}_2\text{L}^4$

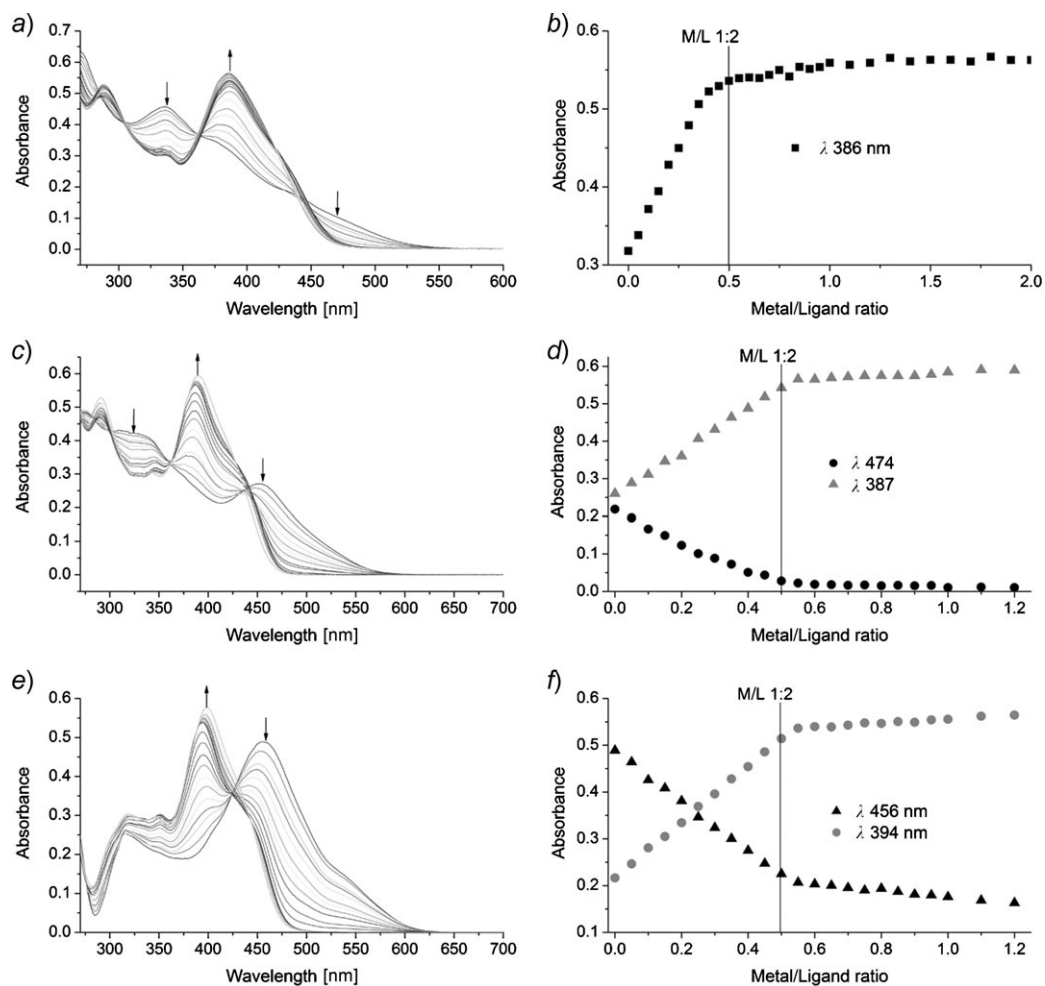


Fig. 4. a) c) e) Change of absorption spectra and b) d) f) absorbance recorded at selected wavelength vs. metal/ligand ratio of the batch titration of ligands with  $\text{Nd}^{3+}$  in DMSO at  $25^\circ$ . a) and b):  $\text{L}^1$ ,  $c = 3.00 \cdot 10^{-5}$  M, 31 batches; c) and d):  $\text{L}^3$ ,  $c = 2.50 \cdot 10^{-5}$  M, 22 batches; e) and f):  $\text{L}^4$ ,  $c = 2.50 \cdot 10^{-5}$  M, 22 batches.

showed a significant change after the addition of  $\text{Et}_3\text{N}$  as an indication of a strong effect of the deprotonation of the ligands on the electronic structure of the molecule, while those of  $\text{H}_2\text{L}^1$  and  $\text{H}_2\text{L}^2$  do not change significantly after addition of  $\text{Et}_3\text{N}$ . From this result, it can be concluded that  $\text{Et}_3\text{N}$  can deprotonate the more acidic  $\text{H}_2\text{L}^3$  and  $\text{H}_2\text{L}^4$  ligands, but it is not sufficiently basic to deprotonate the less acidic  $\text{H}_2\text{L}^1$  and  $\text{H}_2\text{L}^2$  ligands. This trend of the acidities of salophen derivatives is consistent with that of acidities of phenol derivatives (Table 3), and it explains the need for a stronger base such as  $\text{KOH}$  for the spectrophotometric titration of  $\text{H}_2\text{L}^1$ .

From these investigations, we can conclude that these structures in the solid state can be different from those in solution. The structure along with the stoichiometry can



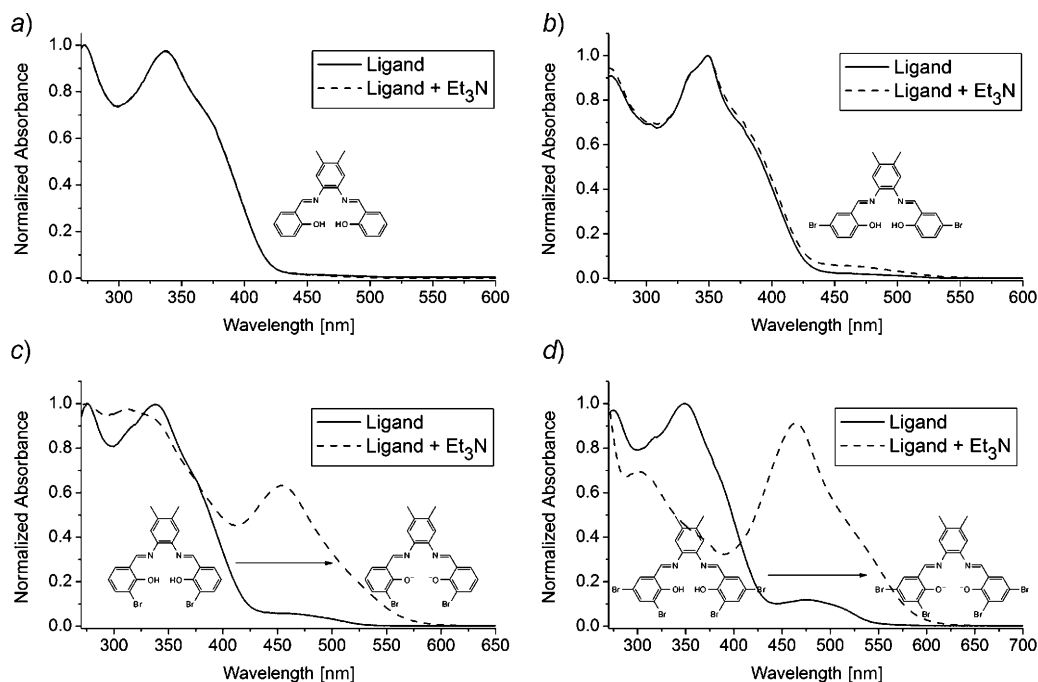
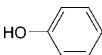
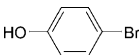
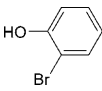
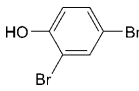


Fig. 5. UV/VIS Absorbance of salophen-type ligands in DMSO without  $Et_3N$  (solid) and with excess  $Et_3N$  (dashed). a)  $H_2L^1$ ,  $c = 3.77 \cdot 10^{-5}$  M; b)  $H_2L^2$ ,  $c = 4.08 \cdot 10^{-5}$  M; c)  $H_2L^3$ ,  $c = 3.92 \cdot 10^{-5}$  M; d)  $H_2L^4$ ,  $c = 3.84 \cdot 10^{-5}$  M.

Table 3.  $pK_a$  Values of Phenol Derivatives [63]

				
Phenol	4-Bromophenol	2-Bromophenol	2,4-Dibromophenol	
$pK_a$	9.994	9.366	8.452	7.790

be controlled by the crystallization conditions. A proper choice of base is the key factor for the stoichiometry of the complex in the solid state. The deprotonation of the ligand can be controlled by the strength of the base and the acidity of the ligand which itself is controlled by the electron-withdrawing effect of the substituents. The protonation state of the ligand is important since it controls the presence or absence of the counter cation for the complex. With a counter cation, an  $[ML_2]^-$  complex is formed because it has a net  $-1$  charge. Without a counter cation, the  $Nd^{3+}$  metal act as counter cation and the  $[M_2L_3]$  complex is formed.

**Luminescence Properties of  $Nd^{3+}$  Complexes in Solution.** The absorption, excitation, and emission spectra of  $[Nd(L^x)_2]^-$  ( $x = 1-4$ ) were recorded in DMSO solution.

For the deprotonation of the ligands, NaOH was used as a base for the creation of these solutions.

The absorption, excitation, and emission spectra of  $[\text{Nd}(\mathbf{L}^1)_2]^-$  are depicted in Fig. 6, a. The apparent maximum of the absorption bands appears around 385 nm. The energy positions of the bands present in the excitation spectra recorded under  $\text{Nd}^{3+}$  signal match closely the position of the bands of the absorption spectra. This result suggests that the NIR-emitting lanthanide cations are sensitized through the electronic levels of the chromophoric ligand and that the ligand is providing an antenna effect. On the basis of their epsilon, we can assess the nature of the electronic bands resulting in the sensitization of  $\text{Nd}^{3+}$  as being  $\pi-\pi^*$ . The NIR-emission spectra reveal the presence of three typical sharp bands arising from the electronic states of  $\text{Nd}^{3+}$ . These bands are located at 900, 1060, and 1330 nm in the NIR region and are attributed to the  ${}^4\text{F}_{3/2} \rightarrow {}^4\text{I}_{9/2}$ ,  ${}^4\text{F}_{3/2} \rightarrow {}^4\text{I}_{11/2}$ , and  ${}^4\text{F}_{3/2} \rightarrow {}^4\text{I}_{13/2}$  f–f transition, respectively.

The other three complexes,  $[\text{Nd}(\mathbf{L}^2)_2]^-$ ,  $[\text{Nd}(\mathbf{L}^3)_2]^-$ , and  $[\text{Nd}(\mathbf{L}^4)_2]^-$ , also show similar absorption, excitation, and emission spectra, which indicate that all these ligands sensitize  $\text{Nd}^{3+}$  (Fig. 6, b–d). However, when the absorption spectra of the four complexes are compared to one another, some red shifts of the maxima of the electronic bands were observed, in the following order:  $[\text{Nd}(\mathbf{L}^1)_2]^- \rightarrow [\text{Nd}(\mathbf{L}^3)_2]^- \rightarrow [\text{Nd}(\mathbf{L}^2)_2]^- \rightarrow [\text{Nd}(\mathbf{L}^4)_2]^-$  (Fig. 7). The excitation spectra also show the same trend of red shift. These results indicate that the more the ligand is substituted by Br-atoms, the more that electronic state is shifted toward lower energy.

To quantify the effect of substituents and to evaluate the efficiency of energy transfer from the sensitizer-ligand to lanthanide and the presence of quenching processes deactivating the  $\text{Nd}^{3+}$  excited state, the quantum yields of the  $\text{Nd}^{3+}$  complexes formed with  $\mathbf{L}^1$ ,  $\mathbf{L}^2$ ,  $\mathbf{L}^3$ , and  $\mathbf{L}^4$  were measured in DMSO with  $\text{K}[\text{Nd}(\text{tropolonato})_4]$  ( $\Phi = 2.1 \cdot 10^{-3}$ ) [40] as a reference. The emission signal of  $\text{Nd}^{3+}$  was monitored, and the excitation was performed upon sensitizer bands. The results are summarized in Table 4. These quantum yields are relatively close to the value obtained for other  $\text{Nd}^{3+}$  complex in DMSO, which is  $2.1 \cdot 10^{-3}$  [40].

Table 4. Quantum Yield ( $\Phi$ ) of  $\text{Nd}^{3+}$  Complexes in DMSO at r.t.

	$\text{Na}[\text{Nd}(\mathbf{L}^1)_2]^{\text{a}}$	$\text{Na}[\text{Nd}(\mathbf{L}^2)_2]^{\text{b}}$	$\text{Na}[\text{Nd}(\mathbf{L}^3)_2]^{\text{c}}$	$\text{Na}[\text{Nd}(\mathbf{L}^4)_2]^{\text{d}}$
Absolute $\Phi_{\text{tot}}$	$1.18 \pm 0.04 \cdot 10^{-3}$	$1.23 \pm 0.08 \cdot 10^{-3}$	$1.6 \pm 0.1 \cdot 10^{-3}$	$2.01 \pm 0.07 \cdot 10^{-3}$

<sup>a)</sup>  $c = 4.95 \cdot 10^{-5}$  M,  $\lambda_{\text{ex}} 385$  nm. <sup>b)</sup>  $c = 8.70 \cdot 10^{-5}$  M,  $\lambda_{\text{ex}} 392$  nm. <sup>c)</sup>  $c = 4.89 \cdot 10^{-5}$  M,  $\lambda_{\text{ex}} 388$  nm. <sup>d)</sup>  $c = 4.99 \cdot 10^{-5}$  M,  $\lambda_{\text{ex}} 395$  nm.

When the quantum yields of the studied complexes are compared, we can notice that the presence of the Br-atoms at the salophen-type ligands enhances the efficiency of the energy transfer from the sensitizer moiety to the  $\text{Nd}^{3+}$ : the greater the number of Br-atoms, the higher the quantum yield. This result can be attributed to an increase in the population of the triplet state due to the heavy-atom effect [64].  $\text{Na}[\text{Nd}(\mathbf{L}^3)_2]$  has a higher quantum yield than  $\text{Na}[\text{Nd}(\mathbf{L}^2)_2]$ , though they have the same number of Br-atoms. Being located in *ortho*-position to the coordinating  $\text{O}^-$ , the Br-atom: 1) has removed a H-atom from that position, *i.e.*, removed a C–H which may cause a

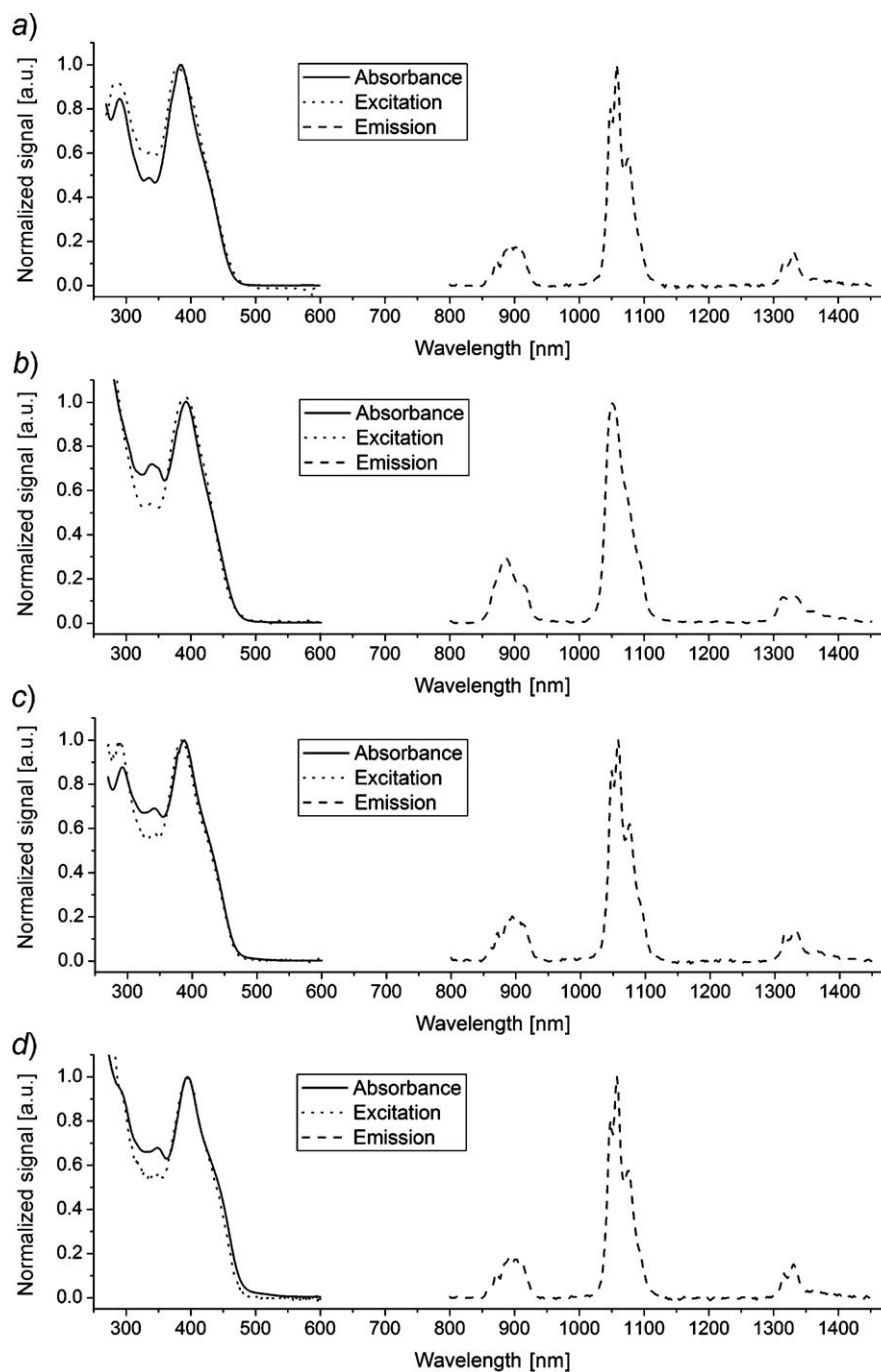


Fig. 6. Absorption (solid), excitation (dotted), and emission (dashed) spectra of  $\text{Na}^+[\text{Nd}(\text{L}^x)_2]^-$  ( $x=1-4$ ) complexes in DMSO at r.t. ( $\lambda_{\text{ex}}$  395 nm for the emission spectrum,  $\lambda_{\text{em}}$  1058 nm for the excitation spectrum). a)  $\text{Na}^+[\text{Nd}(\text{L}^1)_2]^-$ ,  $c = 4.64 \cdot 10^{-5}$  M; b)  $\text{Na}^+[\text{Nd}(\text{L}^2)_2]^-$ ,  $c = 4.65 \cdot 10^{-5}$  M; c)  $\text{Na}^+[\text{Nd}(\text{L}^3)_2]^-$ ,  $c = 4.54 \cdot 10^{-5}$  M; d)  $\text{Na}^+[\text{Nd}(\text{L}^4)_2]^-$ ,  $c = 3.51 \cdot 10^{-5}$  M.

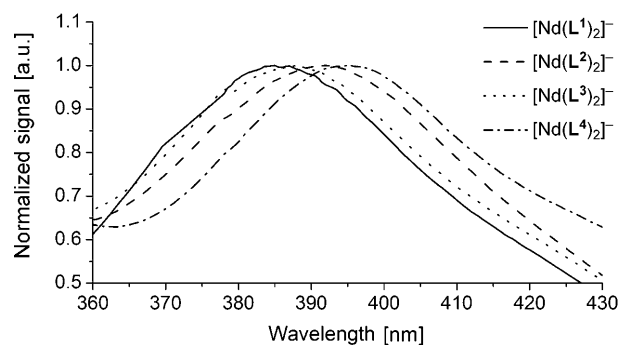


Fig. 7. Comparison of the absorption spectra of the four complexes  $\text{Na}^+[\text{Nd}(\text{L}^x)_2]^-$  ( $x=1-4$ )

nonradiative deactivation of lanthanide luminescence, and 2) has an increased heavy-atom effect by the proximity factor. This conclusion is reinforced by the fact that, since we have not observed important changes of the electronic structures of the chromophores possessing different substituents, the major parameter that explains the different quantum-yield values must be related to the number of Br-substituents through the heavy-atom effect.

The NIR luminescence lifetimes of  $\text{Nd}^{3+}$  in  $\text{Na}[\text{Nd}(\text{L}^1)_2]$ ,  $\text{Na}[\text{Nd}(\text{L}^2)_2]$ , and  $\text{Na}[\text{Nd}(\text{L}^4)_2]$  were measured in DMSO upon ligand excitation (Table 5). The values obtained are all close to a 1.0  $\mu\text{s}$  value. These close lifetime values indicate that the  $\text{Nd}^{3+}$  are all in fairly similar coordination environments in the three different complexes: a similar degree of protection of  $\text{Nd}^{3+}$  is therefore provided by the organization of the ligand around the lanthanide ion. These lifetimes compare well with the luminescence lifetimes previously reported for  $\text{Nd}^{3+}$  complexes (Table 6) [18][24][40]. From this experiment, we got quantitative data showing that the differences in quantum yields cannot be explained by differences in the protection of the NIR-emitting cations.

Table 5. Luminescence Lifetimes ( $\tau$ ) of  $\text{Nd}^{3+}$  Complexes ( $c = 3.7 \cdot 10^{-5}$  M) in DMSO at r.t. The sample was excited at 337 nm with a nitrogen laser, and the signal was collected at 1060 nm.

	$\text{Na}[\text{Nd}(\text{L}^1)_2]$	$\text{Na}[\text{Nd}(\text{L}^2)_2]$	$\text{Na}[\text{Nd}(\text{L}^4)_2]$
$\tau$ [ $\mu\text{s}$ ]	$1.00 \pm 0.01$	$1.01 \pm 0.01$	$0.998 \pm 0.001$

**Conclusions.** – The coordination chemistry and photophysical properties of the  $\text{Nd}^{3+}$  complexes formed with a series of ligands derived from salophen were systematically studied. All these pre-organized rigid tetradentate ligands form well-defined  $[\text{ML}_2]^-$  complexes in solution. We demonstrated that the structures of the complexes in the solid phase can be significantly different from the structures in solution. The morphology of the crystal structure can be controlled by the proper choice of base which itself controls the presence or absence of the counter cations. The spectroscopy studies of the properties of the chromophoric groups of these systems indicate that the different substituents at the ligand do not affect significantly the energies of the different electronic levels. It was established that all four chromophoric

Table 6. Quantum Yields ( $\Phi_{\text{tot}}$ ) and Luminescence Lifetimes ( $\tau$ ) of Relevant Examples of NIR-Emitting  $\text{Nd}^{3+}$  Complexes<sup>a</sup> in DMSO

	$\Phi_{\text{tot}}$	$\tau$ [ $\mu\text{s}$ ]
[Nd( <i>m</i> -terp1)] [18]	N/A	1.2
[Nd( <i>m</i> -terp2)] [18]	N/A	1.2
[Nd(phn) <sub>3</sub> ] [24]	N/A	1.43
[Nd(phn) <sub>4</sub> ] [24]	N/A	1.34
K[Nd(trp) <sub>4</sub> ] [40]	0.0021	1.10

<sup>a</sup> *m*-terp1 = tri-*tert*-butyl 2,2',2''-[(3,3''-bis[(1-butoxypropyl)(phenylcarbonyl)amino]methyl)-5,5',5''-trimethyl-1,1':3',1''-terphenyl-2,2',2''-triy]tris(oxy)]triacetate; *m*-terp2 = tri-*tert*-butyl 2,2',2''-[(3,3''-bis[(1-butoxypropyl)(4-methylphenyl)sulfonyl]amino]methyl)-5,5',5''-trimethyl-1,1':3',1''-terphenyl-2,2',2''-triy]tris(oxy)]triacetate; phn = 9-hydroxyphenalen-1-onato; trp = tropolonato.

ligand systems are able to sensitize  $\text{Nd}^{3+}$ , a NIR-emitting cation, through intramolecular energy transfer from the electronic states of the ligand to the metal ion. The luminescence properties of the complexes can be enhanced by modification of the ligand with Br-substituents.

Funding was provided through the University of Pittsburgh and through the *National Science Foundation* (award DBI0352346). *S. P.* gratefully acknowledges *Le Studium* (Agency for research and international hosting associate researchers in 'Region Centre'), Orléans, France, for financial support.

### Experimental Part

*General.* All reagents and solvents were purchased from the following suppliers and used as received: paraformaldehyde from *Acros Organics*; 5-bromosalicylaldehyde, 4,5-dimethylbenzene-1,2-diamine, and  $\text{MgSO}_4$  from *Aldrich*; 3,5-dibromosalicylaldehyde and trifluoroacetic acid from *Alfa Aesar*;  $\text{CH}_2\text{Cl}_2$ , MeCN, AcOEt, MeOH, THF, and  $\text{Na}_2\text{CO}_3$  from *EMD Chemicals Inc.*;  $\text{Et}_3\text{N}$  from *Fisher Scientific*; AcOH, DMSO,  $\text{Et}_2\text{O}$ , HCl, hexanes, NaOH, and  $\text{MgSO}_4$  from *Mallinckordt Baker, Inc.*; abs. EtOH from *Pharmaco Products, Inc.*;  $\text{Nd}(\text{OTf})_3 \cdot 6 \text{H}_2\text{O}$  from *Strem Chemicals*; 2-bromophenol from *TCI*; all deuterated NMR solvents from *Cambridge Isotope Labs*. M.p.: *Fisher-Johns* melting-point apparatus; uncorrected. IR Spectra: *Perkin-Elmer-Spectrum BX* FT-IR spectrometer; polystyrene film as external standard ( $1601 \text{ cm}^{-1}$  peak);  $\tilde{\nu}$  in  $\text{cm}^{-1}$ .  $^1\text{H-NMR}$  Spectra: *Bruker DPX-300* at 300 MHz;  $\delta$  in ppm,  $J$  in Hz. EI-MS and ESI-MS: *Micromass-Autospec* and *Agilent-HP-1100* LC-MSD, respectively; in  $m/z$ . Elemental analyses were performed by *Atlantic Microlab, Inc.*

*Luminescence Studies.* Absorption spectra: *Perkin-Elmer-Lambda-9* spectrophotometer. Metal-cation luminescence emission and excitation spectra: modified *Jobin-Yvon-Spex Fluorolog-322* spectrofluorometer equipped for both r.t. and 77 K measurements. Luminescence and excitation spectra were corrected for the instrumental function. Metal-cation luminescence quantum yields were measured for the  $^4\text{F}_{3/2} \rightarrow ^4\text{I}_{11/2}$  transition with  $\text{K}[\text{Nd}(\text{tropolonato})_4]$  ( $\Phi = 2.1 \cdot 10^{-3}$  in DMSO) as reference [40]. The use of a  $\text{Nd}^{3+}$  complex allows for a simple method of cross calibrating the VIS detector with the NIR detector of the *Fluorolog-322*. The quantum yields were calculated by *Eqn. 1*, where subscript r stands for the reference and x for the sample;  $A$  is the absorbance at the excitation wavelength,  $I$  is the intensity of the excitation light at the same wavelength,  $\eta$  is the refractive index ( $\eta = 1.479$  in DMSO), and  $D$  is the measured integrated luminescence intensity.

$$\frac{\Phi_x}{\Phi_r} = \frac{A_r(\lambda_r)}{A_x(\lambda_x)} \cdot \frac{I(\lambda_x)}{I(\lambda_r)} \left[ \frac{\eta_x}{\eta_r} \right]^2 \cdot \frac{D_x}{D_r} \quad (1)$$

The luminescence-lifetime measurements were performed by excitation of solns. in 1 cm quartz cells with a nitrogen laser (*Oriel* model 79110, wavelength 337.1 nm, pulse width at half-height 15 ns, 5–30 Hz repetition rate). Emission from the sample was collected at a right angle to the excitation beam by a 3" plano-convex lens. Emission wavelengths were selected by means of quartz filters. The signal was monitored by a cooled photomultiplier (*Hamamatsu R316*) coupled to a 500 MHz bandpass digital oscilloscope (*Tektronix TDS 754D*). The signals (15000 points each trace) from at least 500 flashes were collected and averaged. Background signals were similarly collected and subtracted from sample signals. Lifetimes were averages of at least three independent determinations. Data were fitted with exponential decay curves by OriginPro (V7 SP4) data analysis and linefitting software. Ligand-centered triplet-state lifetimes were performed by excitation of solid samples in a quartz tube at 77 K with the nitrogen laser described above. Emission from the samples was collected at a right angle to the excitation beam, and the emission wavelengths were selected by means of a *Spex-FL-1005* double monochromator. The signal was monitored by a *Hamamatsu-R928* photomultiplier coupled to a 500 MHz bandpass digital oscilloscope (*Tektronix TDS 620B*). The signals (15000 points each trace) from at least 500 flashes were collected and averaged. Background signals were similarly collected and subtracted from sample signals.

*X-Ray Crystallography*<sup>2)</sup>. Crystals suitable for X-ray crystallographic study were coated with *Fluorolube*<sup>®</sup>, then mounted on a glass fiber, and coated with epoxy cement. X-Ray data were collected with a *Bruker-Apex* diffractometer and graphite-monochromatized  $\text{MoK}_\alpha$  radiation ( $\lambda$  0.71073 Å). Data collection was controlled with the *Bruker SMART* program, data processing was done with the *SHELXTL* program package [65], and the graphics were done with *Ortep-3* [66], *Mercury 1.2.1* [67], and *Ortep* [68]. All H-atoms were calculated and placed in idealized positions ( $d(\text{C-H})=0.96$  Å).

*3-Bromosalicylaldehyde* (= *3-Bromo-2-hydroxybenzaldehyde*). To a soln. of  $\text{MgCl}_2$  (2.38 g, 25.0 mmol), paraformaldehyde (2.61 g, 86.8 mmol) and  $\text{Et}_3\text{N}$  (5.00 ml, 3.63 g, 35.9 mmol) in MeCN (50 ml), 2-bromophenol (1.60 ml, 2.39 g, 13.8 mmol) was added. The mixture was refluxed for 2.5 days and then allowed to cool. The soln. was diluted with 1M HCl (80 ml) and extracted with  $\text{Et}_2\text{O}$  ( $3 \times 50$  ml). The org. layer was washed with brine (50 ml), dried ( $\text{MgSO}_4$ ), and concentrated, and the crude product purified by column chromatography (silica gel, 20% AcOEt/hexanes): 3-bromosalicylaldehyde (0.961 g, 35%). <sup>1</sup>H-NMR (300 MHz,  $\text{CDCl}_3$ ): 11.62 (s, OH); 9.88 (s, C(=O)H); 7.79 (dd,  $J=1.5, 7.8, 1$  arom. H); 7.55 (dd,  $J=1.4, 7.7, 1$  arom. H); 6.96 (t,  $J=7.7, 1$  arom. H). EI-MS: 200 ( $M^+$ ,  $\text{C}_7\text{H}_5\text{BrO}_2^+$ ; calc. 199.95).

*2,2'-[(4,5-Dimethyl-1,2-phenylene)bis(nitrilomethylidyne)]bis[phenol]* ( $\text{H}_2\text{L}^1$ ). To a soln. of salicylaldehyde (2.05 g, 16.8 mmol) in EtOH (20 ml), 4,5-dimethylbenzene-1,2-diamine (1.14 g, 8.40 mol) was added. The mixture was heated and sonicated for 15 min ( $\rightarrow$  yellow precipitate). The mixture was filtered and the solid washed with hexanes and dried under vacuum:  $\text{H}_2\text{L}^1$  (2.54 g, 88%). M.p. 144–146°. IR (selected absorbances only; KBr): 1617 (C=N), 1278 (Ar–O). <sup>1</sup>H-NMR (300 MHz,  $\text{CD}_3\text{CN}$ ): 13.22 (s, 2 OH); 8.76 (s, 2 N=CH); 7.50 (dd,  $J=1.6, 7.6, 2$  arom. H); 7.47–7.36 (m, 2 arom. H); 7.19 (s, 2 arom. H); 6.99–6.92 (m, 4 arom. H); 2.32 (s, 2 Me).

*2,2'-[(4,5-Dimethyl-1,2-phenylene)bis(nitrilomethylidyne)]bis[4-bromophenol]* ( $\text{H}_2\text{L}^2$ ). A soln. of 4,5-dimethylbenzene-1,2-diamine (0.160 g, 1.18 mmol) in EtOH (4 ml) was added to a soln. of 3-bromosalicylaldehyde (0.486 g, 2.42 mmol) in EtOH (7 ml). The mixture was refluxed overnight ( $\rightarrow$  orange-yellow precipitate). The mixture was filtered and the solid washed with EtOH and  $\text{Et}_2\text{O}$  and dried under vacuum:  $\text{H}_2\text{L}^2$  (0.506 g, 85%). M.p. 241–245°. IR (KBr): 1616 (C=N), 1277 (Ar–O). <sup>1</sup>H-NMR (300 MHz,  $(\text{D}_6)\text{DMSO}$ ): 8.90 (s, 2 N=CH); 7.86 (d,  $J=2.5, 2$  arom. H); 7.52 (dd,  $J=2.5, 8.8, 2$  arom. H); 7.28 (s, 2 arom. H); 6.92 (d,  $J=8.8, 2$  arom. H); 2.29 (s, 2 Me).

*2,2'-[(4,5-Dimethyl-1,2-phenylene)bis(nitrilomethylidyne)]bis[6-bromophenol]* ( $\text{H}_2\text{L}^3$ ). To a soln. of 3-bromosalicylaldehyde (0.197 g, 0.981 mmol) in EtOH (5 ml), 4,5-dimethylbenzene-1,2-diamine (0.0654 g, 0.480 mmol) was added. The mixture was refluxed for 12 h ( $\rightarrow$  orange precipitate). The mixture was filtered and the solid washed with  $\text{Et}_2\text{O}$  and dried under vacuum:  $\text{H}_2\text{L}^3$  (0.124 g, 51%). <sup>1</sup>H-NMR (300 MHz,  $\text{CD}_3\text{CN}$ ): 8.75 (s, 2 N=CH); 7.67 (dd,  $J=1.6, 7.9, 2$  arom. H); 7.53 (dd,  $J=1.5, 7.7, 2$  arom. H); 7.21 (s, 1 arom. H); 6.91 (t,  $J=7.8, 2$  arom. H); 2.33 (s, 2 Me). EI-MS: 499.974113 ( $M^+$ ,  $\text{C}_{22}\text{H}_{18}\text{Br}_2\text{N}_2\text{O}_2^+$ ; calc. 499.973500).

2) The diffraction studies were carried out by Dr. *Steven Geib*, Department of Chemistry, University of Pittsburgh.

2,2'-[4,5-Dimethyl-1,2-phenylene]bis(nitrilomethylidyne)]bis[4,6-dibromophenol] ( $H_2L^4$ ). To a soln. of 3,5-dibromosalicylaldehyde (1.02 g, 3.66 mmol) in EtOH (15 ml), 4,5-dimethylbenzene-1,2-diamine (0.242 g, 1.78 mmol) was added. The mixture was heated and sonicated for 30 min (→ orange precipitate). The mixture was filtered and the solid washed with hexanes and dried under vacuum:  $H_2L^4$  (1.02 g, 87%).  $^1H$ -NMR (300 MHz,  $(D_6)$ DMSO): 8.97 (s, 2 N=CH); 7.93–7.91 (m, 4 arom. H); 7.36 (s, 2 arom. H); 2.31 (s, 2 Me). EI-MS: 660 ( $M^+$ ,  $C_{22}H_{16}Br_4N_2O_2^+$ ; calc. 659.79).

$Na[Nd(L^1)_2]$ . To a soln. of  $H_2L^1$  (0.115 g, 0.333 mmol) in MeCN (7 ml), a soln. of  $Nd(OTf) \cdot 6 H_2O$  (0.117 g, 0.167 mmol) in MeCN (5 ml) was slowly added. To the resulting soln., 0.1078M NaOH in MeOH (4.6 ml, 0.496 mmol) was then slowly added under stirring. The mixture was refluxed for 2 h. The yellow precipitate was centrifuged, washed with  $Et_2O$ , and dried under vacuum:  $Na[Nd(L^1)_2]$  (0.103 g, 72%). IR (selected absorbances only, KBr): 1618 (C=N), 1544 (C=C), 1385 (Ar–O).

$Na[Nd(L^2)_2]$ . As described for  $Na[Nd(L^1)_2]$ , with  $H_2L^2$  (0.0699 g, 0.139 mmol) in THF (15 ml),  $Nd(OTf) \cdot 6 H_2O$  (0.0487 g, 0.0696 mmol) in MeCN (7.5 ml), and 0.1078M NaOH in MeOH (1.9 ml, 0.209 mmol); reflux for 6 h. The solvents were evaporated, and the residue was triturated with  $Et_2O$ , centrifuged, and dried under vacuum:  $Na[Nd(L^2)_2]$  (0.064 g, 78%). IR (selected absorbances only, KBr): 1616 (C=N), 1522 (C=C), 1373 (Ar–O).

$Na[Nd(L^3)_2]$ . As described for  $Na[Nd(L^1)_2]$ , with  $H_2L^3$  (0.0504 g, 0.100 mmol) in THF (20 ml),  $Nd(OTf) \cdot 6 H_2O$  (0.0351 g, 0.0502 mmol) in MeCN (7 ml), and 0.1078M NaOH in MeOH (1.5 ml, 0.151 mmol); reflux overnight. The solvents were evaporated, and the yellow solid was centrifuged, washed with  $Et_2O$  and dried under vacuum:  $Na[Nd(L^3)_2]$  (0.038 g, 65%).

$Na[Nd(L^4)_2]$ . As described for  $Na[Nd(L^1)_2]$ , with  $H_2L^4$  (0.0534 g; 0.0809 mmol) in THF/MeCN 2 : 1 (v/v; 12 ml),  $Nd(OTf) \cdot 6 H_2O$  (0.0283 g, 0.0405 mmol) in MeCN (3 ml), and 0.1078M NaOH in MeOH (0.13 ml, 0.121 mmol); reflux overnight. The solvents were evaporated, and the yellow solid was centrifuged, washed with  $Et_2O$ , and dried under vacuum:  $Na[Nd(L^4)_2]$  (0.0346 g, 58%).

## REFERENCES

- [1] D. Imbert, M. Cantuel, J.-C. G. Bünzli, G. Bernardinelli, C. Piguet, *J. Am. Chem. Soc.* **2003**, *125*, 15698.
- [2] J.-C. G. Bünzli, C. Piguet, *Chem. Soc. Rev.* **2005**, *34*, 1048.
- [3] J.-C. G. Bünzli, *Acc. Chem. Res.* **2006**, *39*, 53.
- [4] S. Comby, D. Imbert, A.-S. Chauvin, J.-C. G. Bünzli, *Inorg. Chem.* **2006**, *45*, 732.
- [5] R. F. Ziessel, G. Ulrich, L. Charbonnière, D. Imbert, R. Scopelliti, J.-C. G. Bünzli, *Chem. – Eur. J.* **2006**, *12*, 5060.
- [6] S. Comby, D. Imbert, C. Vandevyver, J.-C. G. Bünzli, *Chem. – Eur. J.* **2007**, *13*, 936.
- [7] N. M. Shavaleev, R. Scopelliti, F. Gumy, J.-C. G. Bünzli, *Inorg. Chem.* **2008**, *47*, 9055.
- [8] N. M. Shavaleev, R. Scopelliti, F. Gumy, J.-C. G. Bünzli, *Inorg. Chem.* **2009**, *48*, 2908.
- [9] A. Beeby, R. S. Dickins, S. Faulkner, D. Parker, J. A. G. Williams, *Chem. Commun.* **1997**, 1401.
- [10] C. L. Maupin, D. Parker, J. A. G. Williams, J. P. Riehl, *J. Am. Chem. Soc.* **1998**, *120*, 10563.
- [11] A. Beeby, R. S. Dickins, S. FitzGerald, L. J. Govenlock, D. Parker, J. A. G. Williams, C. L. Maupin, J. P. Riehl, G. Siligardi, *Chem. Commun.* **2000**, 1183.
- [12] S. J. A. Pope, B. J. Coe, S. Faulkner, E. V. Bichenkova, X. Yu, K. T. Douglas, *J. Am. Chem. Soc.* **2004**, *126*, 9490.
- [13] S. J. A. Pope, B. J. Coe, S. Faulkner, R. H. Laye, *Dalton Trans.* **2005**, 1482.
- [14] T. K. Ronson, T. Lazarides, H. Adams, S. J. A. Pope, D. Sykes, S. Faulkner, S. J. Cles, M. B. Hursthouse, W. Clegg, R. W. Harrington, M. D. Ward, *Chem. – Eur. J.* **2006**, *12*, 9299.
- [15] K. Sénéchal-David, S. J. A. Pope, S. Quinn, S. Faulkner, T. Gunnlaugsson, *Inorg. Chem.* **2006**, *45*, 10040.
- [16] T. Lazarides, M. A. H. Alamiry, H. Adams, S. J. A. Pope, S. Faulkner, J. A. Weinstein, M. D. Ward, *Dalton Trans.* **2007**, 1484.
- [17] M. P. Oude Wolbers, F. C. J. M. van Veggel, B. H. M. Snellink-Ruël, J. W. Hofstraat, F. A. J. Geurts, D. N. Reinhoudt, *J. Chem. Soc., Perkin Trans. 2* **1998**, 2141.

- [18] S. I. Klink, G. A. Hebbink, L. Grave, F. G. A. Peters, F. C. J. M. van Veggel, D. N. Reinhoudt, J. W. Hofstraat, *Eur. J. Org. Chem.* **2000**, 1923.
- [19] G. A. Hebbink, L. Grave, L. A. Woldering, D. N. Reinhoudt, F. C. J. M. van Veggel, *J. Phys. Chem. A* **2003**, *107*, 2483.
- [20] M. H. V. Werts, R. H. Woudenberg, P. G. Emmerink, R. van Gassel, J. W. Hofstraat, J. W. Verhoeven, *Angew. Chem.* **2000**, *112*, 4716; *Angew. Chem., Int. Ed.* **2000**, *39*, 4542.
- [21] M. H. V. Werts, J. W. Verhoeven, J. W. Hofstraat, *J. Chem. Soc., Perkin Trans. 2* **2000**, 433.
- [22] R. Van Deun, P. Fias, P. Nockemann, A. Schepers, T. N. Parac-Vogt, K. Van Hecke, L. van Meervelt, K. Binnemans, *Inorg. Chem.* **2004**, *43*, 8461.
- [23] A. P. Bassett, R. Van Deun, P. Nockemann, P. B. Glover, B. M. Kariuki, K. Van Hecke, L. Van Meervelt, Z. Pikamenou, *Inorg. Chem.* **2005**, *44*, 6140.
- [24] R. Van Deun, P. Fias, P. Nockemann, K. Van Hecke, L. Van Meervelt, K. Binnemans, *Inorg. Chem.* **2006**, *45*, 10416.
- [25] R. Van Deun, P. Nockemann, T. N. Parac-Vogt, K. Van Hecke, L. Van Meervelt, C. Görrler-Walrand, K. Binnemans, *Polyhedron* **2007**, *26*, 5441.
- [26] S. Yanagida, Y. Hasegawa, K. Murakoshi, Y. Wada, N. Nakashima, T. Yamanaka, *Coord. Chem. Rev.* **1998**, *171*, 461.
- [27] M. Iwamuro, T. Adachi, Y. Wada, T. Kitamura, N. Nakashima, S. Yanagida, *Bull. Chem. Soc. Jpn.* **2000**, *73*, 1359.
- [28] Y. Hasegawa, T. Ohkubo, K. Sogabe, Y. Kawamura, Y. Wada, N. Nakashima, S. Yanagida, *Angew. Chem.* **2000**, *112*, 365; *Angew. Chem., Int. Ed.* **2000**, *39*, 357.
- [29] Z.-H. Zhang, Y. Song, T. Okamura, Y. Hasegawa, W.-Y. Sun, N. Ueyama, *Inorg. Chem.* **2006**, *45*, 2896.
- [30] Y. Hasegawa, T. Yasuda, K. Nakamura, T. Kawai, *Jpn. J. Appl. Phys.* **2008**, *47*, 1192.
- [31] T. J. Foley, B. S. Harrison, A. S. Knefely, K. A. Abboud, J. R. Reynolds, K. S. Schanze, J. M. Boncella, *Inorg. Chem.* **2003**, *42*, 5023.
- [32] S. Banerjee, L. Huebner, M. D. Romanelli, G. A. Kumar, R. E. Riman, T. J. Emge, J. G. Brennan, *J. Am. Chem. Soc.* **2005**, *127*, 15900.
- [33] L. Bertolo, S. Tamburini, P. A. Vigato, W. Porzio, G. Macchi, F. Meinardi, *Eur. J. Inorg. Chem.* **2006**, 2370.
- [34] L.-N. Sun, J.-B. Yu, G.-L. Zheng, H.-J. Zhang, Q.-G. Meng, C.-Y. Peng, L.-S. Fu, F.-Y. Liu, Y.-N. Yu, *Eur. J. Inorg. Chem.* **2006**, 3962.
- [35] W.-K. Lo, W.-K. Wong, W.-Y. Wong, J. Guo, K.-T. Yeung, Y.-K. Cheng, X. Yang, R. A. Jones, *Inorg. Chem.* **2006**, *45*, 9315.
- [36] E. G. Moore, G. Szigethy, J. Xu, L.-O. Pålsson, A. Beeby, K. N. Raymond, *Angew. Chem., Int. Ed.* **2008**, *47*, 9500.
- [37] M. Giraud, E. S. Andreiadis, A. S. Fisyuk, R. Demadrille, J. Pécaut, D. Imbert, M. Mazzanti, *Inorg. Chem.* **2008**, *47*, 3952.
- [38] S. Quici, M. Cavazzini, G. Marzanni, G. Accorsi, N. Armaroli, B. Ventura, F. Barigelli, *Inorg. Chem.* **2005**, *44*, 529.
- [39] H. Tsukube, Y. Suzuki, D. Paul, Y. Kataoka, S. Shinoda, *Chem. Commun.* **2007**, 2533.
- [40] J. Zhang, P. D. Badger, S. J. Geib, S. Petoud, *Angew. Chem., Int. Ed.* **2005**, *44*, 2508.
- [41] J. Zhang, C. M. Shade, D. A. Chengelis, S. Petoud, *J. Am. Chem. Soc.* **2007**, *129*, 14834.
- [42] J. Zhang, P. D. Badger, S. J. Geib, S. Petoud, *Inorg. Chem.* **2007**, *46*, 6473.
- [43] J. Zhang, S. Petoud, *Chem. – Eur. J.* **2008**, *14*, 1264.
- [44] L. Pellegatti, J. Zhang, B. Drahos, S. Villette, F. Suzenet, G. Guillaumet, S. Petoud, É. Tóth, *Chem. Commun.* **2008**, 6591.
- [45] T. Jüstel, D. U. Wiechert, C. Lau, D. Sendor, U. Kynast, *Adv. Funct. Mater.* **2001**, *11*, 105; T.-S. Kang, B. S. Harrison, T. J. Foley, A. S. Knefely, J. M. Boncella, J. R. Reynolds, K. S. Schanze, *Adv. Mater.* **2003**, *15*, 1093.
- [46] L. H. Sloof, A. Polman, M. P. Oude Wolbers, F. C. J. M. van Veggel, D. N. Reinhoudt, J. W. Hofstraat, *J. Appl. Phys.* **1998**, *83*, 497; L. H. Slooff, A. van Blaaderen, A. Polman, G. A. Hebbink, S. I. Klink, F. C. J. M. Van Veggel, D. N. Reinhoudt, J. W. Hofstraat, *J. Appl. Phys.* **2002**, *91*, 3955.



- [47] S. Stolik, J. A. Delgado, A. Pérez, L. Anasagasti, *J. Photochem. Photobiol., B* **2000**, *57*, 90.
- [48] R. Weissleder, V. Ntziachristos, *Nat. Med.* **2003**, *9*, 123.
- [49] M. G. Muller, I. Georgakoudi, Q. Zhang, J. Wu, M. S. Feld, *Appl. Opt.* **2001**, *40*, 4633.
- [50] T. J. Sweeny, V. Mailander, A. A. Tucker, A. B. Olomu, W. Zhang, Y. Cao, R. S. Negrin, C. H. Contag, *Proc. Natl. Acad. Sci. U.S.A.* **1999**, *96*, 12044.
- [51] Z. Ye, M. Tan, G. Wang, J. Yuan, *Anal. Chem.* **2004**, *76*, 513.
- [52] G. Mathis, *J. Biomol. Screening* **1999**, *4*, 309.
- [53] 'Lanthanide Probes in Life, Chemical and Earth Science: Theory and Practice', Eds. J.-C. G. Bünzli and G. R. Choppin, Elsevier, Amsterdam, 1989.
- [54] S. I. Weissman, *J. Chem. Phys.* **1942**, *10*, 214.
- [55] P. A. Vigato, S. Tamburini, *Coord. Chem. Rev.* **2004**, *248*, 1717.
- [56] R. D. Archer, H. Y. Chen, L. C. Thompson, *Inorg. Chem.* **1998**, *37*, 2089.
- [57] A. J. Gallant, B. O. Patrick, M. J. MacLachlan, *J. Org. Chem.* **2004**, *69*, 8739; A. J. Gallant, J. K.-H. Hui, F. E. Zahariev, Y. A. Wang, M. J. MacLachlan, *J. Org. Chem.* **2005**, *70*, 7936.
- [58] E. Verner, B. A. Katz, J. R. Spencer, D. Allen, J. Hataye, W. Hruzewicz, H. C. Hui, A. Kolesnikov, Y. Li, C. Luong, A. Martelli, K. Radika, R. Rai, M. She, W. Shrader, P. A. Sprengeler, S. Trapp, J. Wang, W. B. Young, R. L. Mackman, *J. Med. Chem.* **2001**, *44*, 2753.
- [59] A. Terzis, D. Mentzafos, H. A. Tajmir-Riahi, *Inorg. Chim. Acta* **1984**, *84*, 187.
- [60] R. D. Shannon, *Acta Crystallogr., Sect. A* **1976**, *32*, 751.
- [61] X. Yang, R. A. Jones, *J. Am. Chem. Soc.* **2005**, *127*, 7686; X.-P. Yang, R. A. Jones, M. M. Oye, A. L. Holmes, W.-K. Wong, *Cryst. Growth Des.* **2006**, *6*, 2122; X. Yang, R. A. Jones, W.-K. Wong, *Dalton Trans.* **2008**, 1676.
- [62] SPECFIT/32, version 3.0.36, Spectrum Software Associates, Marlborough, MA, 1993.
- [63] E. P. Serjeant, B. Dempsey, 'Ionization Constants of Organic Acids in Aqueous Solution', 1st edn., Pergamon Press, New York, 1979.
- [64] S. P. McGlynn, T. Azumi, M. Kinoshita, 'Molecular Spectroscopy of the Triplet State', Prentice-Hall, Englewood Cliffs, NJ, 1969.
- [65] G. M. Sheldrick, SHELXS-97, Program for Crystal Structure Refinement, University of Göttingen, Germany, 1997.
- [66] L. J. Farrugia, *J. Appl. Crystallogr.* **1997**, *30*, 565.
- [67] I. J. Bruno, J. C. Cole, P. R. Edgington, M. Kessler, C. F. Macrae, P. McCabe, J. Pearson, R. Taylor, *Acta Crystallogr., Sect. B* **2002**, *58*, 389.
- [68] P. McArdle, *J. Appl. Crystallogr.* **1995**, *28*, 65.

Received May 4, 2009